Soft Matter

Accepted Manuscript

ROYAL SOCIETY OF CHEMISTRY

www.rsc.org/softmatter

Self-assembly of luminescent *N*-annulated Perylene Tetraesters into Fluid Columnar phases

Ravindra Kumar Gupta,[a] Suraj Kumar Pathak,[a] Balaram Pradhan,[a] D. S. Shankar Rao,[b] S. Krishna Prasad[b] and Ammathnadu S. Achalkumar*[,a]

[a]*Department of Chemistry, Indian Institute of Technology Guwahati, Guwahati, 781039, Assam, India.*
[b] *Centre for Nano and Soft Matter Sciences, Jalahalli, P. B. No. 1329, Bangalore, 560013, India.*

Abstract: A new class of *N*-annulated perylene tetraesters and their *N*-alkylated derivatives have been synthesized. *N*-annulated perylene tetraesters stabilize hexagonal columnar phase over a broad temperature range. Hexagonal columnar phase exhibited by these compounds show good homeotropic alignment with less defects. Annulation in the bay region of perylene tetraesters enhanced the mesophase width in comparison to the parent tetraesters. *N*-alkylation of these compounds perturb the self-assembly behavior and resulting compounds are nonmesomorphic. Bright green luminescence was visually percievable under the long wavelength UV light. All these properties make these materials promising for the application in organic electronics.

Table of contents (TOC) Graphic

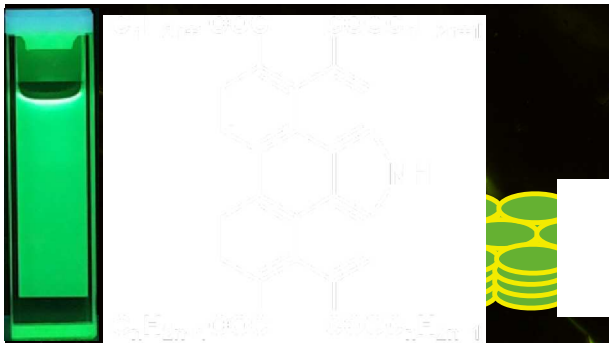

I. Introduction

Perylene derivatives represent an important class of compounds which are widely found application in organic electronics. They are cheap, robust and easily functionalizable chromophores with high band gap, high extinction coefficient and high fluorescence quantum yield. They are also known for their chemical, thermal and photochemical stability.[1] These special properties make them ideal materials to test them in the field of organic solar cells,[2] light emitting diodes[3] and field effect transistors.[4] Perylene based molecules are widely used in the construction of self-assembled supramolecular structures, because of their propensity to aggregate under

various conditions.[5] Introduction of liquid crystallinity in perylene derivatives is a rewarding and challenging task. This is because liquid crystallinity in perylene derivatives ensures a macroscopically ordered self-assembly, while even a minor structural modification drastically perturb the self-assembly and will not guarantee the LC behavior. LC perylene bisimides were reported for the first time in 1997 by Cornier *et. al.*[6a,b] Since then there are many reports on perylene bisimide based liquid crystals obtained either by treatment of perylene bisanhydrides with aromatic or aliphatic amines or by the bay substitution on perylene bisimide core.[6c-k] Bay substitution in perylene derivatives drastically affect the planarity of the molecule which in turn affects the photophysical properties and self-assembly behavior.[7] Recently there is a renewed interest in expanding the aromatic core of perylene derivatives to modulate their structure and properties. Extension along the long axis of perylene bisimides leads to a bathochromic shift, while extension in the bay region leads to a hypsochromic shift.[8] There are reports on the introduction of hetero atoms like nitrogen and sulphur by annulation in the bay region of perylene derivatives which lead to modified aromatic systems with interesting properties.[8,9] Introduction of nitrogen by *N*-annulation in the bay position can provide a possibility to improve the solubility and lower the transition temperature by means of *N*-alkylation.[10] Introduction of nitrogen in the molecular structure leads to hydrogen bonding with the neighboring molecule which may help in the self-assembly.[15b] Liquid crystalline alkylperylene tetracarboxylates are relatively new entrants when compared to LC perylenebisimides.[11,19] Perylene tetraesters are somewhat less electron deficient when compared to perylene bisimides due to the less electron withdrawing ester groups. Because of this they could be used as hole transporting emissive layers in the construction of OLEDs.[6f, 11a, 12, 19] They are known to have higher LUMO and HOMO levels when compared to perylene bisimides which would help to improve the V_{OC} (open circuit voltage) of solar cells.[13] The mesophase width of perylene tetraesters are found to be short, which requires certain structural modification to improve their usability. In this paper, we are reporting new class of luminescent DLCs based on *N*-annulated perylene tetraesters and show that *N*-annulation in the bay region of the perylene tetraesters will help to improve the thermal behavior and emission properties.

II. Results and discussion

II.1 Synthesis and molecular structural characterization

The synthetic route to prepare the target DLCs and their precursors is represented in scheme 1. Perylene-3,4,9,10-tetracarboxylic bisanydride under basic condition hydrolyzed to obtain its tetracarboxylate salt. This salt was acidified with hydrochloric acid to obtain the corresponding tetraacid, which on refluxing in the presence of phase transfer catalyst and *n*-bromoalkanes provided the corresponding tetraesters (**3a-c**) in good yields.[11c-f] The tetraester obtained was subjected to controlled nitration mediated by sodium nitrite in presence of nitric acid to obtain the bay substituted mono nitro derivatives **4a-c** in quantitative yields.[14] These nitro compounds were refluxed in excess triethyl phosphite to yield *N*-annulated perlene tetraesters as bright yellow solids in good yield.[15] Earlier for perylene bisimides *N*-annulation[9] was reported with Buchwald-Hartwig reaction.[16] However we should mention here that, attempts to synthesize bis-*N*-annulated perylene tetraesters from dinitro derivatives were not successful, due to the strain involved in the accommodation of two pyrrole rings in the bay region. Later these *N*-annulated perylene tetraesters (**1a-c**) were *N*-alkylated using sodium hydride as a base to obtain the products (**2a-c**) in 70-80 % yields.[10b] Compounds **2a-c** turned out to be liquids. The structures of all the intermediates and target molecules were confirmed using ^{1}H, ^{13}C NMR, IR spectroscopy and MALDI-TOF analysis. (see the supporting information for the experimental and characterization details).

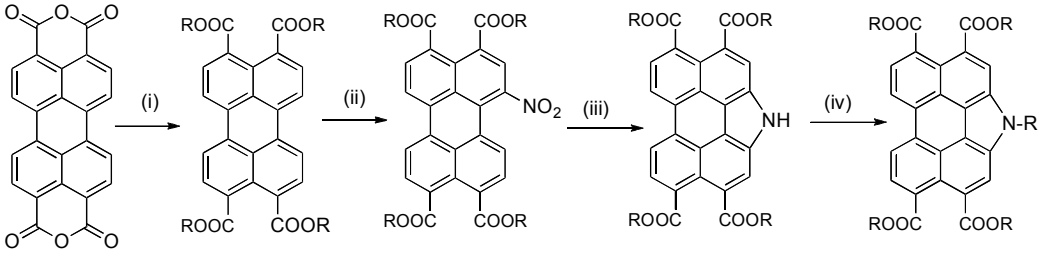

Scheme 1. Synthesis of *N*-annulated perylene tetraesters. Reagents and conditions: i) KOH, H_2O,70 ^{o}C, 0.5 h,1M HCl, Aliquat 336, KI, *n*-bromoalkanes, reflux, 24 h (69-75%); ii) $NaNO_2$, HNO_3,0 ^{o}C, 1 h (80-90%); iii) triethyl phosphite,160 ^{o}C, reflux, 4 h, N_2 (55-60%); iv) NaH, *n*-bromoalkanes, dry THF, reflux, 17 h, N_2 (70-80%)

II. 2. Thermal behavior

The mesomorphism of these new class of DLCs based on *N*-annulated perylene tetraesters (**1a-c**) were investigated by polarizing optical microscope (POM), differential scanning calorimeter (DSC), thermogravimetric analysis (TGA) and X-ray diffraction (XRD) studies. The occurrence of thermotropic LC phase(s) was initially confirmed by POM observation of strong birefringence coupled with fluidity of the compounds. The transition temperatures and associated enthalphies were measured by DSC. The peak temperatures obtained in DSC traces due to phase transitions were found to be concordant with those of POM studies. Further confirmation of LC phase assignment was made according to the characteristic textural pattern observed in POM followed by XRD studies. The transition temperatures and the corresponding enthalpies derived from DSC traces of the first heating-cooling cycles at a rate of 5 ^{o}C/min are provided in table 1. In the following sections, we present the details of LC behaviour of these compounds investigated by using the above-mentioned complementary techniques.

Table 1. Phase transition temperatures [a] (^{o}C) and corresponding enthalpies (kJ/mol) of DLCs

Compound	Phase sequence	
	Heating	Cooling
1a	Cr 91.6 (478.6) Cr 294 (26.6) I	I 281.9 (12.8) Col_h 60.9 (179.9) Cr
1b	Cr 84.51 (565.1) Col_h 273.1 (24.6) I	I 267 (14.6) Col_h 65.3 (213.7) Cr
1c	Cr 103.2 (833) Col_h 201.2 (15.1) I	I 198.8 (11.8) Col_h 76.7 (768.5) Cr

[a] Peak temperatures in the DSC thermograms obtained during the first heating and cooling cycles at 5 ^{o}C/min.

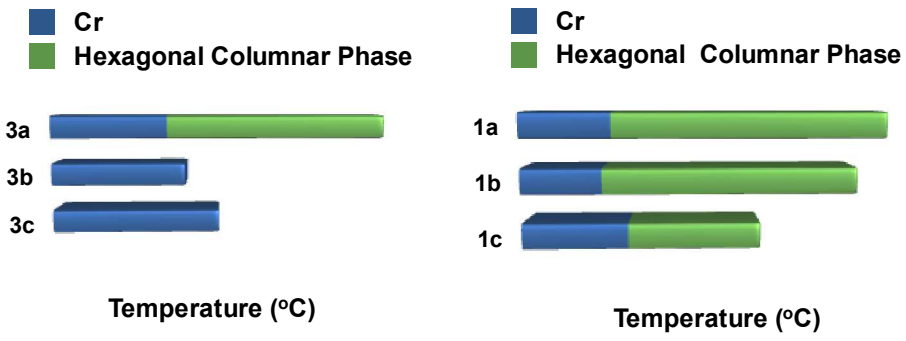

Figure 1. Bargraph summarizing the thermal behavior of compounds **3a-c**[19] and compounds **1a-c** (heating cycle).

All the compounds investigated showed enantiotropic mesomorphic behavior over a broad thermal range. Compound **1a** with *n*-octyloxy tails, exhibited a crystal to mesophase transition at a temperature of 92 ^{o}C with an enthalpy change of 478.6 kJ/mol (Table 1). The transition showed an increase in the birefringence with the sample turning to be fluidic and shearable. The mesophase was spanning over a broad thermal range of 200 degrees and converted into an isotropic liquid at 294 ^{o}C. This wide thermal range over 200 degrees points to a stronger core-core interactions among the adjacent molecules. On cooling the viscous isotropic liquid, large fern leaf like structures started appearing at 282 ^{o}C from the homeotropically aligned area with a dark field of fiew. Further decrease in temperature showed an increase in the birefringence, while the leaf-like structures extended into the existing dark homeotropic domains (Fig. 2a). The mesophase to crystal transition was observed at

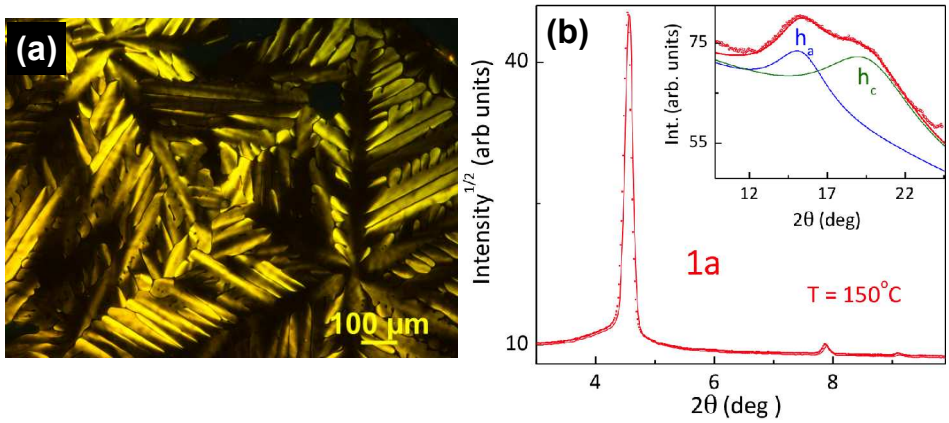

Figure 2. Photomicrograph of compound **1a** at 276 ^{o}C on cooling from isotropic liquid state (a); XRD profiles depicting the intensity against 2θ obtained for the Col$_h$ phase of compound **1a** (b). (h_a and h_c mentioned in the figure corresponds to the stacking of peripheral alkyl chains and central cores respectively)

61 ^{o}C in DSC thermograms (Fig. S26a in SI), with a slight decrease in the birefringence and nonshearability as observed under POM (see SI).

Powder XRD measurements were conducted to determine the symmetry of the thermodynamically stable Col phase formed by compound **1a** at temperature 150 ^{o}C. The results of indexation of the sharp reflections of these XRD profiles to lattices of Col phase are summarized (See Table 1 in SI). The X-ray profile of the Col phase showed (Figure 2b) at 150 ^{o}C showed a strong reflection corresponding to a Bragg spacing *d* of 19.37 Å at low-angle region followed by reflections with *d* spacings of

11.19 Å, 9.69 Å and in the middle-angle region ($7 < 2\theta < 10°$). These reflections are indexed into Miller indices 100, 110, 200 with the ratio 1: $1/\sqrt{3}$: $1/\sqrt{4}$ and thus these values are fitting into the lattice of Col_h phase. In the wide-angle region there are two diffused peaks at 5.78 Å and 4.53 Å, where the first one corresponds to the packing of alkyl chains and the second one corresponding to core-core stacking. The lattice parameter '*a*' calculated was found to be 22.37 Å. This value is approximately 30% less than the diameter obtained from molecular model in it full trans conformation. This can be ascribed to the folding of the flexible chains or possible interdigitation of flexible chains in the neighboring columns.[17]

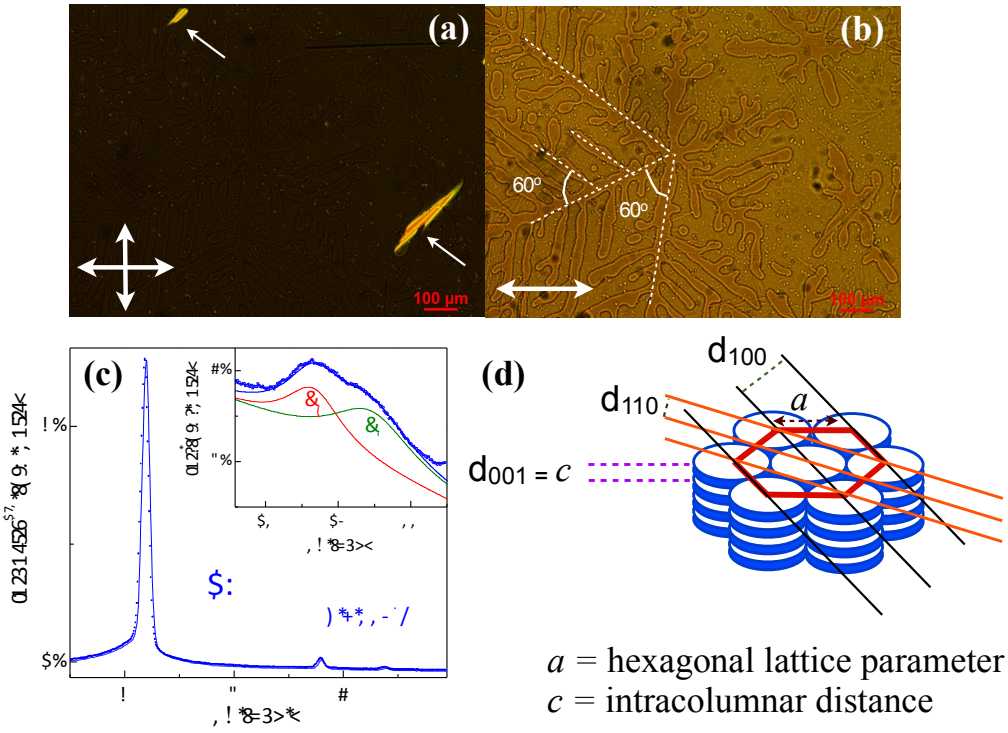

Figure 3. Microscopic images of compound **1b** placed between a glass slide and coverslip on slow cooling (1°C/min) from the isotropic phase at 195 °C (a) with crossed polarizers and (b) with parallel polarizers (dashed lines indicate the growth directions of the dendritic structures; the arrows indicate linear defects in the homeotropic alignment); (c) XRD profiles depicting the intensity against 2θ obtained for the Col_h phase of compound **1b**; (d) Schematic of hexagonal columnar (Col_h) phase.

Compound **Ib** with *n*-decyloxy tails placed between two untreated glass substrates, on heating showed a crystal to mesophase melting transition as evidenced

by DSC at about ≈85 °C with an enthalpy change of 565.1 kJ/mol (See Fig.S26b). The mesophase transforms into isotropic liquid at 273 ^{o}C. Cooling the isotropic liquid at a rate of 5 ^{o}C/min showed the homeotropic alignment with a dark field of view under crossed polarizers. Homeotropically aligned Col phase between cross-polarizers typically do not show birefringence in POM, because in this case, the optical axis is in alignment with the columnar axis (Fig 3a).[18] When the polarizers are parallel the texture shows hexagonal dendritic domains (Fig. 3b). Further cooling results in the developments of fern leaf like structures from homeotropically-aligned domains. The branching of the dendritic growth starts with a 60^{o} angle to the main axis[18e,f,g] as shown in the figure 3b. This feature is a characteristic of a highly ordered hexagonal columnar phase. The homeotropic alignment where the individual column is oriented perpendicular to the substrate is an essential feature, for the construction of organic photovoltaics.[18c] In homeotropic alignment, the first molecule aligns with its face-on to the substrate over which the incoming molecules stack one above the other regularly to give a highly ordered column of indefinite length (Fig. 4c). Most of the reported DLCs does not attain homeotropic alignment over a large area, instead they align homogeneously (edge-on) or with partial homeotropic alignment. In the case of homogeneous or edge-on alignment the discotic molecules are stacked with their sides on the surface (Fig. 4d), which is the requirement for the fabrication of field effect transistors. It has been reported that presence of hetero atoms at the periphery of the molecules help them to attain homeotropic alignment on polar surfaces.[18d] Thus the *N*-annulation at the bay position helps in inducing homeotropic alignment. Further, there is a possibility that nitrogen atom of one molecule may form H-bonding with the hydrogen attached to the nitrogen of another molecule. This can happen with another molecule present in the next plane of the same column as shown in Figure 4a or it can also happen with another molecule from the other column in the same plane as shown in Figure 4b. This also supports the homeotropic alignment of columns over indefinite lengths. Presence of intermolecular H-bonding is evident as seen by the lowering of N-H stretching frequency in IR to 3353 cm^{-1} (SI).

The diffractogram of the compound **1b** at 250 ^{o}C (Table 1 in SI) showed one sharp reflection at *d* spacing 20.28 Å at low angle ($2\theta \approx 4.4°$), two reflections at with *d* spacings of 11.71 Å, 10.14 Å in the middle-angle region ($7° < 2\theta < 11°$). These reflections along with the two diffused halos at wide angle can be indexed into a

lattice of hexagonal Col phase with the Miller indices 100, 110, 200 in the ratio 1: 1/√3: 1/√4. Two diffused peaks are observed at a *d* spacing of 5.82 Å and 4.73 Å, corresponds to the packing of flexible tails and the stacking of the discs within the column. Diffraction patterns obtained at lower temperature (227 ^{o}C and 100 ^{o}C) showed that Col_h phase is not undergoing any transition to the other variant of Col phase with different symmetry (Fig.3c and Table 1 in SI).

Compound **1c** with *n*-dodecyloxy tails shows a crystal to mesophase transition centered at 103 ^{o}C with an enthalpy change of 833 kJ/mol and it turns to isotropic liquid at 201 ^{o}C. The mesophase range is reduced when compared to its lower homologues **1a** and **1b**. On cooling the isotropic liquid the mesophase starts appearing at 199 ^{o}C with large homeotropic domains interspersed with very few linear defects. It

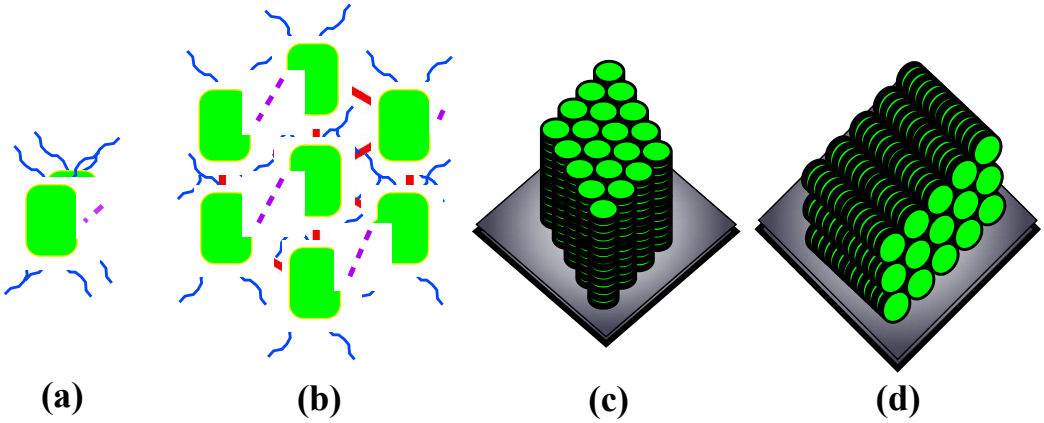

Figure 4. Schematics showing the intermolecular H-bonding between the molecules from two different planes (a) and within a plane (b); Schematic representation of (c) homeotropic (face-on) alignment and (d) homogeneous (edge-on) alignment

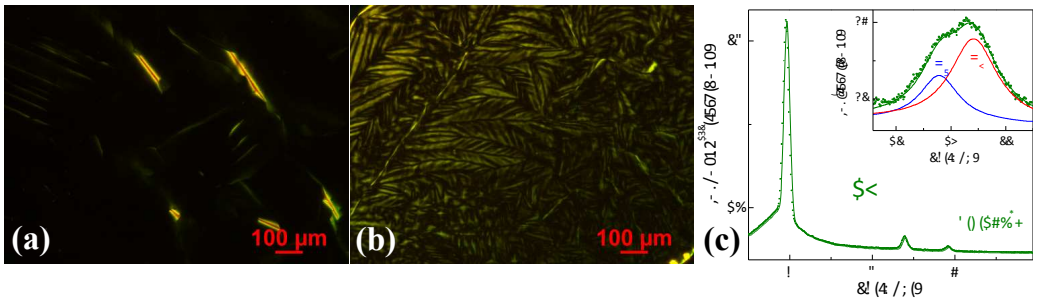

Figure 5. Microphotographs of compound **1c** obtained on slow cooling (1°C/min) from the isotropic phase at 182 °C (a); at 102 ^{o}C (b); XRD profiles depicting the intensity against 2θ obtained for the Col_h phase of compound **1c** at 180 ^{o}C (c).

is possible to obtain a defect free homeotropic alignment by slow cooling (at a rate of 1°C/min) of the isotropic liquid (Fig. 5a). On cooling further a fibrous texture was obtained (Fig. 5b) and remains unaltered even after the crystallization temperature at 78 °C. X-ray diffraction studies carried out at different temperature intervals suggested that the mesophase observed is a Col phase with hexagonal symmetry (Table 1 in SI). All the XRD patterns revealed the presence of one intense and two medium intensity peaks at low angle region followed by two diffused peaks at wide angles (Fig. 6c). The first three *d* spacings are indexed into Miller indices 100, 110, 200 with the typical ratio of 1: 1/√3: 1/√4 corresponding to a columnar hexagonal lattice. The first diffused peak was corresponding to the packing of flexible alkyl chains and the second diffused peak was corresponding to the packing of discs. From high temperature (180 °C) to low temperature (150 °C) the intercolumnar distance '*a*' reduced from 25.97 Å to 25.79 Å, with the concurrent decrease in the core-core distance from 4.65 Å to 4.61 Å. Thus all the molecules investigated exhibited ordered Col_h phase over a wide range. These compounds have a propensity to align homeotropically on a glass surface on slow cooling. With the increase in the chain length the mesophase range was reduced because of the lowering of clearing temperatures. When compared to the simple perylene tetraesters **3a-c** (**3a** was enatiotropic, while **3b** and **3c** were monotropic LCs), the annulated compounds **1a-c** were enantiotropic with broad mesophase range (Fig. 1). This enhanced mesophase stability is probably attributed to the presence of –NH- at the bay position.

Stability of the compounds has been determined by TGA and it has been shown that these compounds were stable up to at least 300 °C and complete decomposition occurs at 550 °C (see SI). As mentioned earlier these *N*-alkylated derivatives **2a-c** lost their ability to self-assemble into Col architecture, because of the presence of alkyl tails, which may prevent the stacking.

III. Photophysical properties

Photophysical properties of these *N*-annulated perylene tetraesters in solution are depicted in table 2. Absorption and fluorescence spectra of the compounds **1a-c** and **2a-c** were taken in micromolar solutions in THF. Representative spectra for

compound **1a** and **2a** are given in Fig. 6. As can be seen, the absorption spectra obtained for the solutions of **1a-c** showed a single absorption maximum centered at 459 nm, with two shoulder peaks at 434 nm and 410 nm. Compounds **2a-c**, which are the *N*-alkylated derivatives of compounds **1a-c** showed single absorption maximum at 462 nm with a shoulder peak at 436 nm. The molar absorption coefficients were calculated and found that the values were comparable to the molar absorption coefficient of perylene tetraester (**1a-c**: ε = >10,500 $M^{-1}cm^{-1}$; **2a-c**: ε = >14,600 $M^{-1}cm^{-1}$; **3a**: ε = >14,800 $M^{-1}cm^{-1}$). Both the series of molecules exhibited a hypsochromic shift when compared to corresponding tetraester **3a**. Emission spectra of compounds **1a-c** obtained by exciting

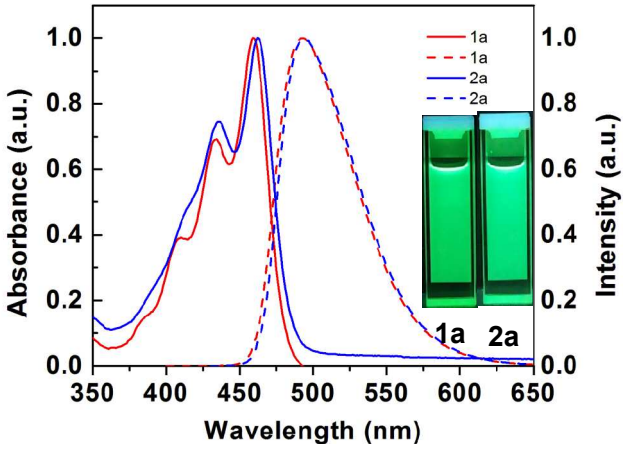

Figure 6. (a) Absorption (LHS) and emission (RHS) spectra in micromolar THF solution for compounds **1a** and **2a**. Inset shows the pictures of micromolar THF solutions as seen under the UV illumination of wavelength 365 nm.

Table 2. Photophysical[a] properties

Entry	Absorption[b]	Emission[b,c]	Stokes shift[b]	$\Delta E^{d,e}_{g,\,opt}$	Quantum Yield[f]
1a	459,434,410	492	33	2.48	1
1b	459,434,410	495	36	2.48	0.97
1c	459,434,410	493	34	2.48	0.98
2a	462,435	494	32	2.48	0.97
2b	462,436	494	32	2.48	0.86
2c	462,436	492	30	2.48	0.88
3a	470,441	489, 517	19	2.46	1

[a] in micromolar solutions in THF; [b] wavelengths (nm); [c] the excitation wavelength λ_{ex} = λ_{max} of each compound (459 nm for **1a-c**, 462 nm for **2a-c**, 470 nm for **3a**); [d] calculated from the red edge of the absorption band (501 nm for **1a-2c**; 504 nm for **3a**); [e] in eV; [f] Relative quantum yield calculated with respect to fluorescein solution in 0.1 M NaOH with a quantum yield of 0.79.

the solutions of these compounds at their absorption maxima showed emission with their emission maxima centered around 492-495 nm with a Stoke's shift of 33-36 nm. Compounds **2a-c** also exhibited similar emission spectra with their emission maxima centered at 492-494 nm with a Stoke's shift of 30-32 nm. While the emission spectra of tetraester **3a** showed an emission maximum at 489 nm with a shoulder at 517 nm. The Stoke's shift found was 19 nm, which is lower than **1a-c** and **2a-c** (Table 2, see the SI). Length of alkyl chain does not influence emission spectra of these molecules.[11b, 20] Solutions of both these compounds exhibit bright green fluorescence under UV light of long wavelength as shown in figure 6 (inset). Absorption and emission spectra of these compounds showed concentration dependence. UV-Vis absorption and emission spectra of Compounds **1a** and **2a** were taken as a function of concentration (SI, Fig. S32). Dilution of the micromolar solution yielded similar absorption spectra except a reduction in the intensity. Emission spectra obtained after dilution also showed a similar trend. All the compounds **1a-c** and **2a-c** showed high fluorescence quantum yields (Table 2, SI) and they can be used as standards for quantum yield measurement because of their high solubility in organic solvents (at wavelengths 459-462 nm). [21]

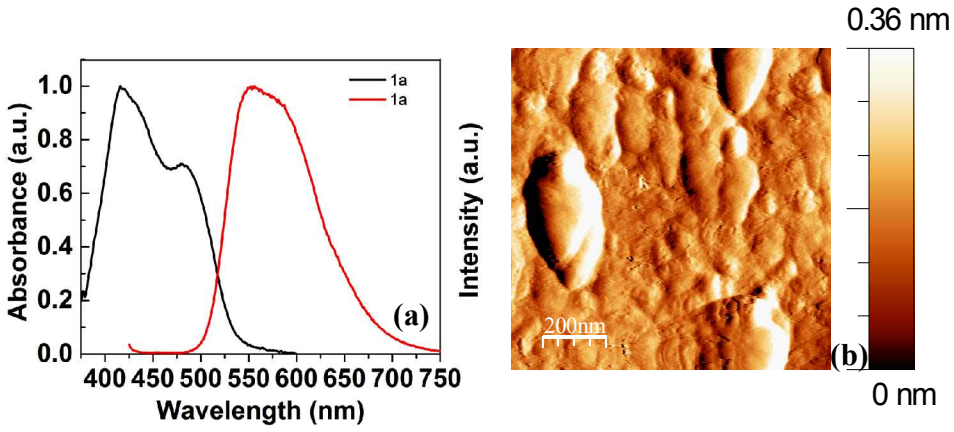

Figure 7. (a) Absorption (black trace) and emission (red trace) spectra obtained for the spin coated thin film for compound **1a**; (b) AFM topography of the spin coated film of compound **1a**

Micromolar solutions of compound **1a** in toluene were used to prepare the thin film on glass slide by spin coating (500-2000 rpm). The absorption and emission

spectra of this film were measured. The absorption spectrum obtained showed two maxima at 416 nm and 479 nm respectively, while the emission spectrum showed a single maximum at 556 nm. The absorption and emission spectrum in the solid state has shown a red shift with a Stoke's shift of 77 nm (Fig.7a). The red shifted absorption and emission maxima are due to the formation of J-aggregates, where the molecules are arranged in a head to tail fashion in aggregates.[14, 22] Thin film showed orange luminescence under the UV light of 365 nm wavelength. AFM imaging of the same film was carried out to examine the film morphology, which showed the presence of aggregates (Fig. 7b). Thin film of the sample was prepared also by sandwiching the sample **1a** and shearing it in isotropic state. The sample was cooled and on cooling it showed the characteristic texture for Col_h phase. Suddenly the sample was frozen to ~ 0 ^oC and once again the POM image was taken. This frozen sample showed the characteristic texture corresponding to Col_h phase. On irradiation with the UV light of 365 nm wavelength, orange fluorescence was observed (See Fig.S31). This shows that the compound is fluorescing even in Col_h phase and its fluorescence is not quenched due to the self-assembly.

In order to get further insights into this anisotropic molecular system and to compare it with the simple perylene core, fluorescence lifetime and steady state anisotropy were measured in dilute solution (3μM) of compound **1a** in ethanol. The measured lifetime was found to be around 3.6 ns (SI) which is lower as compared to the measured life time value reported for perylene which is 5.2 ns in ethanol solution.[23] The decreased fluorescence lifetime could be attributed to higher non-radiative rate due to a change in shape and size of the molecules and thus molecular interactions. The steady state anisotropy value for compound **1b** was found to be 0.185. This value is higher than the one obtained for perylene tetraester, which could be due to the enhanced shape anisotropy of this molecule.[11f]

IV. Cyclic Voltammetry

Cyclic voltammetry (CV) gives valuable information and allows the estimation of frontier molecular orbitals (HOMO and LUMO levels) and band gap of the organic materials. *N*-annulated perylene tetraester **1a**, *N*-alkylated derivative **2a** and tetraester **3a** were investigated by carrying out cyclic voltammetry studies in

micromolar THF solution. The energy levels and band gaps calculated from these studies are tabulated in table 3. A 0.1 M solution of tetrabutylammonium perchlorate (TBAP) was used as a supporting electrolyte in deoxygenated THF. A single compartment cell equipped with $Ag/AgNO_{3\ (0.1M)}$ reference electrode, platinum rod counter electrode and glassy carbon working electrode was used for the experiments. The reference electrode was calibrated with the ferrocene/ferrocenium (Fc/Fc^{+}) redox couple (with absolute energy level of –4.80 eV with respect to vacuum).[24] The cyclic voltammograms were recorded with a scanning rate of 0.05 mVs^{-1}.

Table 3. Electrochemical[a] properties

Entry	$\lambda_{max\ (nm)}$	$\lambda_{onset\ (nm)}$	$\Delta E^{b,c}{}_{UV}$	$E^{d}{}_{1red}$	$E^{d}{}_{1oxd}$	$E^{b,e}{}_{HOMO}$	$E^{b,f}{}_{LUMO}$	$\Delta E^{b,g}{}_{g,\ CV}$
1a	459	501	2.48	-1.02	0.92	-5.16	-3.22	1.94
2a	459	501	2.48	-1.03	0.97	-5.21	-3.21	2.0
3a	459	504	2.46	-1.04	0.89	-5.13	-3.2	1.93

[a] Experimental conditions: $Ag/AgNO_3$ as reference electrode, Platinum rod working electrode, Glassy carbon wire counter electrode, TBAP (0.1 M) as a supporting electrolyte, room temperature, [b] In electron volts (eV), [c] Band gap determined from the red edge of the longest wave length in the UV-vis absorption spectra, [d] In volts (V), [e] Estimated from the formula $E_{HOMO} = -(-4.8 + E_{1/2,\ Fc,Fc^{+}} - E_{oxd,\ onset})$eV , [f]Estimated from the onset reduction peak values by using $E_{LUMO} = -(4.8 - E_{1/2,\ Fc,Fc^{+}} + E_{red,\ onset})$eV. [g]Estimated from the formula $\Delta E_{g,\ CV} = E_{HOMO} - E_{LUMO}$.

All the compounds exhibited well-defined irreversible oxidation and reduction waves (See SI). The optical band gap $E_{g,opt}$ was estimated from the red edge of the absorption spectra (Table 4). *N*-annulated perylene tetraester **1a** and their *N*-alkylated derivative **2a** exhibited same band gaps. Energy levels LUMO were determined by using the formula $E_{LUMO} = -(4.8 - E_{1/2,\ Fc,Fc^{+}} + E_{red,\ onset})$ eV, while HOMO energy levels were determined by using the formula $E_{HOMO} = -(-4.8 + E_{1/2,\ Fc,Fc^{+}} - E_{oxd,\ onset})$ eV Compounds **1a, 2a** and **3a** exhibited LUMO levels -3.22 eV, -3.21 eV and -3.2 eV, and HOMO levels -5.16 eV, -5.21 eV and -5.13 eV respectively (Table 4). Thus the bandgaps obtained for these compounds were almost similar.

V. Experimental Section

Commercially available chemicals were used without any purification; solvents were dried following the standard procedures. Chromatography was performed using either silica gel (60-120 and 100-200) or neutral alumina. For thin layer chromatography (TLC), pre-coated aluminum sheets with silica gel were

employed. IR spectra were obtained on a Perkin Elmer IR spectrometer at room temperature by using KBr pellet. The spectral positions are given in wave number (cm^{-1}) unit. NMR spectra were recorded using Varian Mercury 400 MHz (at 298K) or Bruker 600 MHz NMR spectrometer. For ^{1}H NMR spectra, the chemical shifts are reported in ppm relative to TMS as an internal standard. Coupling constants are given in Hz. Mass spectra were determined from MALDI-TOF mass spectrometer using α-cyanocinnamic acid as a matrix or High Resolution Mass Spectrometer. The mesogenic compounds were investigated for their liquid crystalline behavior (birefringence and fluidity) by employing a polarizing optical microscope (POM) (Nikon Eclipse LV100POL) equipped with a programmable hot stage (Mettler Toledo FP90). Clean glass slides and glass coverslips were employed for the polarizing optical microscopic observations. The transition temperatures and associated enthalpy changes were determined by differential scanning calorimeter (DSC) (Mettler Toledo DSC1) under nitrogen atmosphere. Peak temperatures obtained in DSC corresponding to transitions were in agreement with the polarizing optical microscopic observations. The transition temperatures obtained from calorimetric measurements of the first heating and cooling cycles at a rate of 5 °C/min are tabulated. In the cases where the DSC signatures are not observed for the phase transitions, the transition temperatures have been taken from microscopic observations. Temperature dependent X-ray diffraction studies were carried on unaligned powder samples in Lindemann capillaries (1mm diameter) held in programmable hot stage and irradiated with CuKα radiation (λ = 1.5418 Å). The samples were filled in the capillary tube in their isotropic state and their both ends were flame sealed. The apparatus essentially consisted of a high-resolution powder X-ray diffractometer (Xenocs) equipped with a focusing elliptical mirror and a high-resolution fast detector. Thermogravimetric analysis (TGA) was performed using thermogravimetric analyzer (Mettler Toledo, model TG/SDTA 851 e) under a nitrogen flow at a heating rate of 10 °C/min. UV-Vis spectra were obtained by using Perkin-Elmer Lambda 750, UV/VIS/NIR spectrometer. Fluorescence emission spectra in solution state were recorded with Horiba Fluoromax-4 fluorescence spectrophotometer or Perkin Elmer LS 50B spectrometer. Cyclic Voltammetry studies were performed using a Versa Stat 3 (Princeton Applied Research) Electrochemical workstation.

VI. Summary

In summary, we have synthesized new class of luminescent dicotics based on *N*-annulated perylene tetraesters and their *N*-alkylated derivatives. The length of their peripheral alkyl chains were varied to understand their effect on their thermal behavior. These compounds were thoroughly characterized and investigated for their thermal and photophysical properties. The thermal behavior was studied with the help of POM, DSC, TGA and powder XRD studies.

N-annulated perylene tetraesters stabilized ordered columnar phases with hexagonal symmetry over a broad thermal range. These molecules have propensity to align homeotropically over a large area which is very important from the technological viewpoint. The observed value of hexagonal lattice parameter '*a*' was less than the calculated molecular diameter, probably due to the folding or interdigitation of the peripheral alkyl tails. With the increase in the flexible chain length the mesophase range decreases due to the reduction in the clearing temperature. Increase in chain length shows an increase in the lattice parameter '*a*'. TGA studies have shown that these molecules are stable up to at least 300 ^{o}C. *N*-alkylated derivatives of these compounds did not stabilize liquid crystalline phase showing that presence of –NH- at the bay region is essential for the liquid crystallinity. This may create additional stabilizing factor for the Col self-assembly and homeotropic alignment of these molecules. This structural modification also enhanced the mesophase range of these compounds when compared to the perylene tetraesters.

These molecules show visually percievable green light emission in solution. These are low bandgap materials as evidenced from their absorption spectra with a bandgap of 2.48 eV. *N*-alkylation of *N*-annulated perylene tetraesters does not change the absorption and emission behavior of the molecules. Length of the peripheral chains does not have much imapct on their photophysical properties. Cyclic voltammetry studies have shown that *N*-annulated perylene tetraesters and their *N*-alkylated derivatives do not vary large from perylene tetraesters. This promising class of DLCs with the ease of synthesis, broad range Col_h phase, green light emission and low bandgap can be potential candidates for the fabrication of OLEDs. Finally this

series of molecules open up a new area to explore the structure-property relationships in various novel bay annulated perylene derivatives.

VII. Associated Content

The synthesis and charcterization details, ^{1}H NMR, ^{13}C NMR spectra of all new compounds, absoroption and emission spectra, POM photographs, DSC thermograms, XRD profiles of LC compounds, TGA curves, and Cyclic voltammograms are provided as electronic supporting information. This material is available free of charge via the Internet.

Acknowledgements

ASA sincerely thanks Science and Engineering Board (SERB), DST, Govt. of India and BRNS-DAE for funding this work through the project No. SB/S1/PC-37/2012 and No. 2012/34/31/BRNS/1039 respectively. We thank the Ministry of Human Resource Development for Centre of Excellence in FAST (F. No. 5-7/2014-TS-VII). ASA acknowledges CIF, IIT Guwahati for analytical facilities. We acknowledge Dr. Chandan Mukherjee, IIT Guwahati for providing his Electrochemical work station and Dr. Santanu Kumar Pal for providing fluorescence life time and steady state anisotropy measurements.

References

1 (a) C. W. Tang, *Appl. Phys. Lett.* 1986, **48**, 183–185. (b) L. Schmidt-Mende, A. Fechtenkötter, K. Müllen, E. Moons, R. H. Friend, J. D. MacKenzie, *Science* 2001, **293**, 1119–1122. (c) X. Zhan, Z. Tan, B. Domercq, Z. An, X. Zhang, S. Barlow, Y. Li, D. Zhu, B. Kippelen, S. R. Marder, *J. Am. Chem. Soc.* 2007, **129**, 7246–7247.

2 (a) A. Mishra, M. K. R. Fischer, P. Bäuerle, *Angew. Chem. Int. Ed.* 2009, **48**, 2474–2499. (b) C. Li, M. Liu, N. G. Pschirer, M. Baumgaten, K. Müllen, *Chem. Rev.* 2010, **110**, 6817–6855.

3 (a) A. C. Grimsdale, K. L. Chan, R. E. Martin, P. G. Jokisz, A. B. Holmes, *Chem. Rev.* 2009, **109**, 897–1091. (b) C. Zhong, F. Duan, H. Wu, Y. Cao, *Chem. Mater.* 2011, **23**, 326–340.

4 (a) J. Zaumseil, H. Sirringhaus, *Chem. Rev.* 2007, **107**, 1296–1323. (b) W. Wu, Y. Liu, D. Zhu, *Chem. Soc. Rev.* 2010, **39**, 1489–1502.

5 (a) F. Würthner, C. Thalacker, A. Sautter, *Adv. Mater.* 1999, **11**, 754-758. (b) F. Würthner, A. Sautter, *Chem. Commun.* 2000, 445- 446. (c) F. Würthner, C.

Thalacker, A. Sautter, C. Thalacker, *Angew. Chem., Int. Ed.* 2000, **39**, 1243-1245. (d) A. P. H. J. Schenning, J. van Herrikhuyzen, P. Ionkheijm, Z. Chen, F. Würthner, E. W. Meijer, *J. Am. Chem. Soc.* 2002, **124**, 10252-10253. (e) R. Dobrawa, F. Würthner, *Chem. Commun.* 2002, 1878-1879. (f) T. van der Boom, R. T. Hayes, Y. Zhao, P. J. Bushard, E. A. Weiss, M. R. Wasielewski, *J. Am. Chem. Soc.* 2002, **124**, 9582-9590. (g) E. Peeters, P. A. van Hal, C. J. Meskers, R. A. J. Janssen, E. W. Meijer, *Chem. Eur. J.* 2002, **8**, 4470-4474. (h) C.-C. You, F. Würthner, *J. Am. Chem. Soc.* 2003, **125**, 9716-9725. (i) Z. Chen, V. Stepanenko, V. Dehm, P. Prins, L. D. A. Siebbeles, J. Seibt, P. Marquetand, V. Engel, F. Würthner, *Chem. Eur. J.* 2007, **13**, 436–449. (j) X. Zhang, S. Rehm, M. M. Safont-Sempere, F. Würthner, *Nature Chemistry* 2009, **1**, 623–629. (k) D. Görl, X. Zhang, F. Würthner, *Angew. Chem. Int. Ed.* 2012, **51**, 6328–6348. (l) M. Funahashi, *J. Mater. Chem. C*. 2014, **2**, 7451–7459.

6 (a) R. A. Cornier, B. A. Gregg, *J. Phys. Chem. B* 1997, **101**, 11004-11006. (b) R. A. Cornier, B. A. Gregg, *Chem. Mater.* 1998, **10**, 1309-1319. (c) C. W. Struijk, A. B. Sieval, J. E. J. Dakhorst, M. van Dijk, P. Kimkes, R. B. M. Koehorst, H. Donker, T. J. Schaafsma, S. J. Picken, A. M. van de Craats, J. M. Warman, H. Zuilhof, E. J. R. Sudhölter, *J. Am. Chem. Soc.* 2000, **122**, 11057-11066. (d) I. Seguy, P. Destruel, H. Bock, *Synthetic Metals* 2000, **111**, 15–18. (e) F. Würthner, C. Thalacker, S. Diele, C. Tschierske, *Chem. Eur. J.* 2001, **7**, 2245-2253. (f) S. Alibert-Fouet, S. Dardel, H. Bock, M. Oukachmih, S. Archambeau, I. Seguy, P. Jolinat, P. Destruel, *ChemPhysChem.* 2003, **4**, 983-985. (g) F. Würthner, *Chem. Commun.* 2004, 1564-1579; (h) B. Jancy, S. K. Asha, *J. Phys. Chem. B*. 2006, **110**, 20937–20947. (i) V. Dehm, Z. Chen, U. Baumeister, P. Prins, L. D. A. Siebbeles, F. Würthner, *Org. Lett.* 2007, **9**, 1085–1088. (j) B. Jancy, S. K. Asha, *Chem. Mater.* 2008, **20**, 169–181. (k) G. A. Bhavsar, S. K. Asha, *Chem. Eur. J.* 2011, **17**, 12646–12658.

7 (a) S. Leroy-Lhez, J. Baffreau, L. Perrin, E. Levillain, M. Allain, M. Blesa, P. Hudhomme, *J. Org. Chem*. 2005, **70**, 6313-6320. (b) Z. Chen, M. G. Debije, T. Debaerdemaeker, P. Osswald, F. Würthner, *ChemPhysChem* 2004, **5**, 137-140. (c) L. Schmidt-Mende, A. Fechtenkotter, K. Müllen, E. Moons, R. H. Friend, J. D. Mackenzie, *Science* 2001, **293**, 1119–1122. (d) C. Ego, D. Marsitzky, S. Becker, J. Zhang, A. C. Grimsdale, K. Müllen, J. D. Mackenzie, C. Silva, R. H. Friend, *J. Am. Chem. Soc.* 2003, **125**, 437–443. (e) B. A. Jones, M. J. Ahrens, M. Yoon, A. Facchetti, T. J. Marks, M. R. Wasielewski, *Angew. Chem. Int. Ed.* 2004, **43**, 6363–6366. (f) R. Schmidt, M. M. Ling, J. H. Oh, M. Winkler, M. Konemann, Z. Bao, F. Würthner, *Adv. Mater.* 2007, **19**, 3692–3695.

8 H. Qian, C. Liu, Z. Wang, D. Zhu, *Chem. Commun.* 2006, 4587–4589.

9 H. Qian, W. Yue, Y. Zhen, S. Di Motta, E. Di Donato, F. Negri, J. Qu, W. Xu, D. Zhu, Z. Wang, *J. Org. Chem.* 2009, **74**, 6275–6282.

10 (a) Y. Zhen, H. Qian, J. Xiang, J. Qu, Z. Wang, *Org. Lett.* 2009, **11**, 3084–3087. (b) Y. Li, Z. Wang, *Org. Lett.* 2009, **11**, 1385–1387. (c) H. Chen, C. He, G. Yu, Y. Zhao, J. Huang, M. Zhu, H. Liu, Y. Guo, Y. Li, Y. Liu, *J. Mater. Chem.* 2012, **22**, 3696-3698.

11 (a) T. Hassheider, S. A. Benning, H.-S. Kitzerow, M.-F. Achard, H. Bock, *Angew. Chem. Int. Ed.* 2001, **40**, 2060–2063. (b) S. Benning, H.-S. Kitzerow, H. Bock, M.-F. Achard, *Liq. Cryst.* 2000, **27**, 901–906. (c) X. Mo, H.-Z. Chen, M.-M. Shi, M. Wang, *Chemical Physics Letters* 2006, **417**, 457–460. (d) C. Xue, R. Sun, R. Annab, D. Abadi, S. Jin, *Tetrahedron Lett.* 2009, **50**, 853-856. (e) A. Wicklein, M.-A. Muth, M. Thelakkat, *J. Mater. Chem.* 2010, **20**, 8646–8652. (f) S. K. Gupta, S. Setia, S. Sidiq, M. Gupta, S. Kumar, S. K. Pal, *RSC Adv.* 2013, **3**, 12060-12065.

12 (a) I. Seguy, P. Jolinat, P. Destruel, R. Mamy, H. Allouchi, C. Courseille, M. Cotrait, H. Bock, *ChemPhysChem* 2001, 448-452. (b) I. Seguy, P. Jolinat, P. Destruel, J. Farenc, R. Mamy, H. Bock, J. Ip, T.P. Nguyen, *J. Appl. Phys.* 2001**,** **89**, 5442–5448.

13 Y. Jiang, L. Lu, M. Yang, C. Zhan, Z. Xie, F. Verpoort, S. Xiao, *Polym. Chem.* 2013, **4**, 5612-5620.

14 C. V. Yelamaggad, A. S. Achalkumar, D. S. S. Rao, S. K. Prasad, *J. Org. Chem.* 2007, **72**, 8308–8318.

15 J. J. Looker, *J. Org. Chem.* 1972, **37**, 3379-3381. (b) W. Jiang, H. Qian, Y. Li, Z. Wang, *J. Org. Chem.* 2008, **73**, 7369–7372.

16 (a) J. F. Hartwig, *In Handbook of Organopalladium Chemistry for Organic Synthesis*; E. I. Negishi, A. de Meijere, Eds.; Wiley-Interscience: Weinheim, Germany, 2002. (b) L. Jiang, S. L. Buchwald, In *Metal-Catalyzed Cross-Coupling Reactions*, 2nd ed.; A. de Meijere, F. Diederich, Eds.; John Wiley & Sons: Weinheim, Germany, 2004.

17 (a) V. Percec, C.-H. Ahn, T. K. Bera, G. Ungar, D. J. P. Yeardley, *Chem. Eur. J.* 1999, **5**, 1070–1083. (b) S. K. Pathak, R. K. Gupta, S. Nath, D. S. Shankar Rao, S. Krishna Prasad, A. S. Achalkumar, *J. Mater. Chem. C*, 2015, DOI: 10.1039/c5tc00009b

18 (a) S. Segeyev, W. Pisula, Y. H. Geerts, *Chem. Soc. Rev.* 2007, **36**, 1902−1929. (b) J. Eccher, G. C. Faria, H. Bock, H. von Seggern, I. H. Bechtold, *ACS Appl Mater Interfaces* 2013, **5**, 11935–11943. (c) C. Simpson, J. Wu, M. Watson, K. Mullen, *J. Mat. Chem.* 2004, **14**, 494–504. (d) K. Hatsusaka, K. Ohta, I. Yamamoto, H. Shirai, *J. Mater. Chem.* 2001, **11**, 423-433; (e) W. Pisula, Z. Tomovic, B. El Hamaoui, M. D. Watson, T. Pakula, K. Müllen, *Adv. Funct. Mater.* 2005, **15**, 893−904. (f) T. Yang, J. Pu, J. Zhang, and W. Wang, *J. Org. Chem.* 2013, **78**, 4857–4866. *(g)* P. Oswald, *J. Phys. France* 1988*,* **49***,* 1083-1089.

19 X. Mo, M. -M. Shi, J. -C. Huang, M. Wang, H. -Z. Chen, *Dyes and Pigments*, 2008, **76**, 236-242.

20 P. Uznanski, S. Marguet, D. Markovitsi, P. Schuhmacher, H. Ringsdorf, *Mol. Cryst. Liq. Cryst.*1997, **293**, 123-133.

21 A. M. Brouwer, *Pure Appl. Chem*. 2011, **83**, 12, 2213–2228.

22 (a) M. Kasha, H. R. Rawls, M. A. El- Bayoumi, *Pure Appl. Chem.* 1965, **11**, 371-392. (b) D. D. Prabhu, N. S. S. Kumar, A. P. Sivadas, S. Varghese, and S. Das, *J Phys Chem B*, 2012, **116**, 13071–13080. (c) A. S. Achalkumar, U. S. Hiremath, D.

S. Shankar Rao, S. Krishna Prasad, C. V. Yelamaggad, *J. Org. Chem.* 2013, **78**, 527−544.

23 L. B.-A. Johansson, H. Langhals, *Spectrochimica Acta A*, 1991, **47A**, 857-861.

24 (a) Y. Li, Y. Cao, J. Gao, D. Wang, G. Yu, A. J. Heeger, *Synth. Met*. 1999, **99**, 243–248. (b) C.V. Yelamaggad, A. S. Achalkumar, D. S. Shankar Rao, S. K. Prasad, *Org. Lett*. 2007, **9**, 2641–2644.